ICAS-88-5.7R

EFFECT OF AERODYNAMIC HEATING ON DEFORMATION OF COMPOSITE CYLINDRICAL PANELS IN A GAS FLOW

Victor Birman
Dept. of Naval Architecture and Marine Engineering
University of New Orleans
New Orleans, Louisiana, USA

Charles W. Bert
School of Aerospace and Mechanical Engineering
University of Oklahoma
Norman, Oklahoma, USA

Isaac Elishakoff
Dept. of Aeronautical Engineering
Technion - Israel Institute of Technology
Haifa, Israel

Abstract

In this paper motions of composite cylindrical panels in a gas flow are considered. It is shown that the main factor contributing to large static deformations is a nonuniform aerodynamic heating, while aerodynamic pressure is of secondary importance, at high Mach number.

It turns out that the main factor resulting in the increase of deformations is the nonuniform distribution of temperature along the curved edges. Deformations decrease rapidly in shallower panels. Nonuniformly heated panels become unstable at the values of axial compressive load which are much smaller than the static buckling value calculated in the absence of temperature. The condition of panel flutter of nonuniformly heated composite panels in a gas flow is also formulated.

I. Introduction

Problems of panel flutter of composite cylindrical shells have been studied since the seventies.[1-3] At high flight velocities and with modern materials, aerodynamic heating has to be included in the analysis. The effect of temperature on supersonic panel flutter of aerospace structures was studied in references 4-8.

In this paper the effect of aerodynamic heating on the behavior of a simply supported composite cylindrical panel in a supersonic gas flow is considered. Both aerodynamic and material damping effects are neglected. The aerodynamic pressure is described by piston theory. The temperature distribution is assumed to be a general quadratic function of both the x and the y position coordinates:

$$T = (a_o + a_1 x + a_2 x^2)(b_o + b_1 y + b_2 y^2)\, T_o$$

This assumption permits reduction to uniform, linear, and parabolic distributions of the temperature in particular cases.

It is shown that cylindrical panels experience static deformations in a nonuniform thermal field. These deformations can exist even if the gas flow is absent. The presence of a gas flow can result in panel flutter, superimposed on static deformations. The effects of different geometries, temperature distributions, and axial compression on static deformations of nonuniformly heated panels are considered in numerical examples.

II. Analysis

Consider a cylindrical panel in a supersonic gas flow (Fig. 1). The axial length of the panel is a, the arc length of the curved edges is b, and the radius of the middle surface is R. The panel is formed of layers symmetrically oriented with respect to the middle surface. The number of layers is large so that the analysis can utilize the assumption that the panel is orthotropic. The analysis is based on Donnell's shell theory, which was shown to be sufficiently accurate for thin, shallow composite shells that are not too long.[9]

Then the equations of motion of the panel can be written in terms of displacements and thermal and external forces as follows:

$$L_{11}u + L_{12}v + L_{13}w - N_{x,x}^T - N_{xy,y}^T = 0$$

$$L_{12}u + L_{22}v + L_{23}w - N_{xy,x}^T - N_{y,y}^T = 0$$

$$L_{13}u + L_{23}v + L_{33}w - N_1 w_{,xx} - N_2 w_{,yy} = q - \rho h \ddot{w} \quad (1)$$

where u, v, and w denote the axial, circumferential, and radial displacements, respectively; N_x^T, N_y^T, N_{xy}^T are thermal stress resultants; N_1 and N_2 are the stress resultants of external loads acting in the x and y directions, respectively; ρ is the mean density of the material; h is the total panel thickness; and q is the intensity of aerodynamic loading. The differential operators L_{ij} corresponding to the generalization of Donnell's theory to orthotropic shells are[9]

$$L_{11} = A_{11}d_x^2 + A_{66}d_y^2 \;;\; L_{12} = (A_{12}+A_{66})d_x d_y$$

$$L_{13} = (A_{12}/R)d_x \;;\; L_{22} = A_{66}d_x^2 + A_{22}d_y^2$$

$$L_{23} = (A_{22}/R)d_y$$

$$L_{33} = D_{11}d_x^4 + 2(D_{12}+2D_{66})d_x^2 d_y^2 + D_{22}d_y^4 + A_{22}/R \quad (2)$$

In equations (2), A_{ij} and D_{ij} are extensional and bending stiffnesses, respectively; d_x and d_y denote differentiations with respect to the corresponding argument.

Following the well-known piston theory, one can represent the aerodynamic pressure as

$$q = -\frac{\rho_a c^2 M^2}{\sqrt{M^2-1}}\, w_{,x} \quad (3)$$

where ρ_a is the gas density, c is the sound velocity in the gas, and M is the Mach number. The vector of thermal stress resultants is given by

$$N^T = \sum_{k=1}^{N} Q^{(k)} \alpha^{(k)} h_k \, T \quad (4)$$

where

$$N^T = \begin{Bmatrix} N_x^T \\ N_y^T \\ N_{xy}^T \end{Bmatrix} \qquad \alpha^{(k)} = \begin{Bmatrix} \alpha_x \\ \alpha_y \\ \alpha_{xy} \end{Bmatrix}_k$$

$$Q^{(k)} = \begin{bmatrix} Q_{11} & Q_{12} & Q_{16} \\ Q_{12} & Q_{22} & Q_{26} \\ Q_{16} & Q_{26} & Q_{66} \end{bmatrix}_k \tag{5}$$

Here $Q^{(k)}$ is the matrix of the transformed plane-stress reduced stiffnesses of the k-th layer, $\alpha^{(k)}$ is the vector of the transformed thermal expansion coefficients of the same layer, and T is the temperature which is assumed to be independent of time. The total number of layers is N, the thickness of the k-th layer is h_k.

The relationships between the elements of the vector $\alpha^{(k)}$ and α_L and α_T, the coefficients of thermal expansion in the principal orthotropic directions of the layer are:

$$\begin{aligned} \alpha_x &= \alpha_L \cos^2\theta + \alpha_T \sin^2\theta \\ \alpha_y &= \alpha_L \sin^2\theta + \alpha_T \cos^2\theta \\ \alpha_{xy} &= (\alpha_L - \alpha_T) \sin\theta \cos\theta \end{aligned} \tag{6}$$

where θ is the lamination angle.

The temperature distribution is assumed to be a general quadratic function of the middle-surface coordinates:

$$T = (a_o + a_1 x + a_2 x^2)(b_o + b_1 y + b_2 y^2) T_o \tag{7}$$

This assumption permits consideration of uniform, linear and parabolic distributions, in particular cases.

$$N^T = \beta T \tag{8}$$

where

$$\beta = \begin{Bmatrix} \beta_1 \\ \beta_2 \\ \beta_6 \end{Bmatrix} \tag{9}$$

is the vector of reduced thermal stiffness coefficients

$$\beta = \sum_{k=1}^{N} Q^{(k)} \alpha^{(k)} h_k \tag{10}$$

The boundary conditions at the edges x = 0, x = a, y = 0, and y = b correspond to S2 conditions in the terminology of Almroth.[10] These conditions are satisfied if the displacements field is represented by the following series:

$$\begin{aligned} u &= \sum_n (U_{1n} \cos\frac{\pi x}{a} + U_{2n} \cos\frac{2\pi x}{a}) \sin\frac{n\pi y}{b} \\ v &= \sum_n (V_{1n} \sin\frac{\pi x}{a} + V_{2n} \sin\frac{2\pi x}{a}) \cos\frac{n\pi y}{b} \\ w &= \sum_n (W_{1n} \sin\frac{\pi x}{a} + W_{2n} \sin\frac{2\pi x}{a}) \sin\frac{n\pi y}{b} \end{aligned} \tag{11}$$

The substitution of equations (11) into the first two equations (1) and applying the Galerkin procedure yield the following two independent sets of algebraic equations.

$$\begin{aligned} k_1 \bar{U}_{1n} + k_2 \bar{V}_{1n} &= k_3 \bar{W}_{1n} + T_1 \\ k_2 \bar{U}_{1n} + k_4 \bar{V}_{1n} &= k_5 \bar{W}_{1n} + T_2 \end{aligned} \tag{12}$$

and

$$\begin{aligned} k_6 \bar{U}_{2n} + k_7 \bar{V}_{2n} &= k_8 \bar{W}_{2n} + T_3 \\ k_7 \bar{U}_{2n} + k_9 \bar{V}_{2n} &= k_{10} \bar{W}_{2n} + T_4 \end{aligned} \tag{13}$$

where

$$(\bar{U}_{1n}, \bar{V}_{1n}, \bar{U}_{2n}, \bar{V}_{2n}) = (U_{1n}, V_{1n}, U_{2n}, V_{2n})/h \tag{14}$$

are the nondimensional amplitudes of in-surface displacements. The nondimensional coefficients k_i in equations (12,13) are

$$\begin{aligned} k_1 &= (\pi\bar{h})^2 \bar{A}_{11} + (n\pi\lambda\bar{h})^2 \bar{A}_{66} \\ k_2 &= n\lambda(\pi\bar{h})^2 (\bar{A}_{12} + \bar{A}_{66}) \quad ; \quad k_3 = \pi\bar{a}\bar{h}^2 \bar{A}_{12} \\ k_4 &= (\pi\bar{h})^2 \bar{A}_{66} + (n\pi\lambda\bar{h})^2 \bar{A}_{22} \quad ; \quad k_5 = n\pi\lambda\bar{a}\bar{h}^2 \bar{A}_{22} \\ k_6 &= (2\pi\bar{h})^2 \bar{A}_{11} + (n\pi\lambda\bar{h})^2 \bar{A}_{66} \\ k_7 &= 2k_2 \quad ; \quad k_8 = 2k_3 \\ k_9 &= (2\pi\bar{h})^2 \bar{A}_{66} + (n\pi\lambda\bar{h})^2 \bar{A}_{22} \quad ; \quad k_{10} = k_5 \end{aligned} \tag{15}$$

where

$$\bar{a} = a/R \quad , \quad \bar{h} = h/a \quad , \quad \lambda = a/b \tag{16}$$

and

$$\bar{A}_{ij} = A_{ij}/E_T h \tag{17}$$

E_T being the transverse-direction modulus of elasticity of a layer. The nondimensional thermal terms in equations (12,13) are given by the following relations:

$$\begin{aligned} T_1 &= 8\bar{h}\{2(a_2 a^2)[b_o f_1(n) + b_1 b f_2(n) + b_2 b^2 f_3(n)] \\ &\quad + \lambda(a_1 a + a_2 a^2)[b_1 b f_1(n) + 2b_2 b^2 f_2(n)]\bar{\beta}_3\}/\pi \\ T_2 &= -8\bar{h}\{\lambda\bar{\beta}_2[2a_o + a_1 a + a_2 a^2(1 - 4/\pi^2)][b_2 b^2 f_4(n)] \\ &\quad + \bar{\beta}_3(-a_1 a + a_2 a^2)[b_1 b f_4(n) + b_2 b^2 f_5(n)]\}/\pi \\ T_3 &= -2(\lambda/\pi^2)\bar{h}(a_2 a^2)[b_1 b f_1(n) + 2b_2 b^2 f_2(n)]\bar{\beta}_3 \end{aligned}$$

$$T_4 = 4\bar{h}\{\lambda\bar{\beta}_2(a_1 a + a_2 a^2)[b_2 b^2 f_4(n)] + \bar{\beta}_3(a_2 a^2) \cdot [b_1 b f_4(n) + b_2 b^2 f_5(n)]\}/\pi \quad (18)$$

where

$$(\bar{\beta}_1, \bar{\beta}_2, \bar{\beta}_3) = (\beta_1, \beta_2, \beta_3)\ (T_o/E_T h) \quad (19)$$

are nondimensional parameters and

$$f_1(n) = (1 - \cos n\pi)/n\pi$$

$$f_2(n) = -(\cos n\pi)/n\pi$$

$$f_3(n) = -2/(n\pi)^3 - [1/(n\pi) - 2/(n\pi)^3] \cos n\pi \quad (20)$$

$$f_4(n) = (\cos n\pi - 1)/(n\pi)^2 \; ; \; f_5(n) = 2 \cos n\pi/(n\pi)^2$$

Note that the products $a_1 a$, $a_2 a^2$, $b_1 b$, and $b_2 b^2$ are nondimensional parameters.

From equations (12,13) the nondimensional in-surface amplitudes can be expressed in terms of $\bar{W}_{1n}$ and $\bar{W}_{2n}$:

$$\begin{aligned} \bar{U}_{1n} &= S_1 \bar{W}_{1n} + S_2 \\ \bar{V}_{1n} &= S_3 \bar{W}_{1n} + S_4 \\ \bar{U}_{2n} &= S_5 \bar{W}_{2n} + S_6 \\ \bar{V}_{2n} &= S_7 \bar{W}_{2n} + S_8 \end{aligned} \quad (21)$$

where

$$\begin{aligned} S_1 &= (k_3 k_4 - k_2 k_5)/(k_1 k_4 - k_2^2) \\ S_2 &= (k_4 T_1 - k_2 T_2)/(k_1 k_4 - k_2^2) \\ S_3 &= (k_1 k_5 - k_2 k_3)/(k_1 k_4 - k_2^2) \\ S_4 &= (k_1 T_2 - k_2 T_1)/(k_1 k_4 - k_2^2) \\ S_5 &= (k_8 k_9 - k_7 k_{10})/(k_6 k_9 - k_7^2) \\ S_6 &= (k_9 T_3 - k_7 T_4)/(k_6 k_9 - k_7^2) \\ S_7 &= (k_6 k_{10} - k_7 k_8)/(k_6 k_9 - k_7^2) \\ S_8 &= (k_6 T_4 - k_7 T_3)/(k_6 k_9 - k_7^2) \end{aligned} \quad (22)$$

The substitution of equations (3) and (11) into the third equations (1) and applying again the Galerkin procedure yield the set of differential equations:

$$\begin{aligned} (\rho h^2/E_T)\ddot{\bar{W}}_{1n} + k_{11}\bar{U}_{1n} + k_{12}\bar{V}_{1n} + k_{13}\bar{W}_{1n} &= k_{14}\bar{W}_{2n}\bar{M} \\ (\rho h^2/E_T)\ddot{\bar{W}}_{2n} + k_{15}\bar{U}_{2n} + k_{16}\bar{V}_{2n} + k_{17}\bar{W}_{2n} &= k_{18}\bar{W}_{1n}\bar{M} \end{aligned} \quad (23)$$

In equations (23)

$$\bar{M} = M^2/\sqrt{M^2 - 1} \quad (24)$$

The nondimensional coefficients are given by

$$\begin{aligned} k_{11} &= -\pi\bar{a}\bar{h}^2\bar{A}_{12} = -k_3 \\ k_{12} &= -n\pi\lambda\bar{a}\bar{h}^2\bar{A}_{22} = -k_5 \\ k_{13} &= (\pi\bar{h})^4[\bar{D}_{11} + 2(\bar{D}_{12} + 2\bar{D}_{66})(n\lambda)^2 + \bar{D}_{22}(n\lambda)^4] \\ &\quad + (\bar{a}\bar{h})^2 A_{22} + \bar{N}_1 + (n\lambda)^2\bar{N}_2 \\ k_{14} &= (8/3)\bar{h}(\rho_a c^2/E_T) \\ k_{15} &= 2k_{11} \; ; \; k_{16} = k_{12} \\ k_{17} &= (\pi\bar{h})^4[16\bar{D}_{11} + 8(\bar{D}_{12} + 2\bar{D}_{66})(n\lambda)^2 + D_{22}(n\lambda)^4] \\ &\quad + (\bar{a}\bar{h})^2\bar{A}_{22} + 4\bar{N}_1 + (n\lambda)^2\bar{N}_2 \\ k_{18} &= -k_{14} \end{aligned} \quad (25)$$

where

$$\bar{D}_{ij} = D_{ij}/E_T h^3 \quad (26)$$

and

$$\bar{N}_i = (\tfrac{\pi}{a})^2 N_i h/E_T \qquad (i = 1,2) \quad (27)$$

is the nondimensional axial load.

Equations (23) can be written in terms of radial deflections only:

$$\begin{aligned} (\rho h^2/E_T)\ddot{\bar{W}}_{1n} + R_1\bar{W}_{1n} + R_2 &= k_{14}\bar{M}\,\bar{W}_{2n} \\ (\rho h^2/E_T)\ddot{\bar{W}}_{2n} + R_3\bar{W}_{2n} + R_4 &= k_{18}\bar{M}\,\bar{W}_{1n} \end{aligned} \quad (28)$$

where

$$\begin{aligned} R_1 &= k_{11}S_1 + k_{12}S_3 + k_{13} \\ R_2 &= k_{11}S_2 + k_{12}S_4 \\ R_3 &= k_{15}S_5 + k_{16}S_7 + k_{17} \\ R_4 &= k_{15}S_6 + k_{16}S_8 \end{aligned} \quad (29)$$

The solution of equations (28) consists of static and dynamic parts:

$$\begin{aligned} \bar{W}_{1n} &= \bar{W}_{1n}^{\,o} + \bar{W}_{1n}^{\,t} \sin \omega t \\ \bar{W}_{2n} &= \bar{W}_{2n}^{\,o} + \bar{W}_{2n}^{\,t} \sin \omega t \end{aligned} \quad (30)$$

where ω is the frequency of harmonic vibrations of the fluttering panel.

The substitution of equations (30) into equations (28) yields two independent sets of algebraic equations. The solution of the set including the static deflections is

$$\begin{aligned} \bar{W}_{1n}^{\,o} &= \frac{(R_2 + k_{14}R_4/R_3)\bar{M}}{(k_{14}k_{18}/R_3)\bar{M}^2 - R_1} \\ \bar{W}_{2n}^{\,o} &= (k_{18}\bar{M}/R_3)\bar{W}_{1n}^{\,o} - R_4/R_3 \end{aligned} \quad (31)$$

The set including the dynamic deformations can be written in the form:

$$(R_1 - \bar{\omega}^2)\bar{W}_{1n}^{\,t} - k_{14}\bar{M}\,\bar{W}_{2n}^{\,t} = 0$$

$$-k_{18}\bar{M}\,\bar{W}_{1n}^{t} - (R_3 - \bar{\omega}^2)\bar{W}_{2n}^{t} = 0 \qquad (32)$$

where

$$\bar{\omega}^2 = \rho h^2\omega^2/E_T \qquad (33)$$

The Mach number parameter $\bar{M}$ corresponding to the flutter oscillations of the panel is obtained from equation (32) as

$$\bar{M} = \sqrt{(R_1 - \bar{\omega}^2)(R_3 - \bar{\omega}^2)/(-k_{14}k_{18})} \qquad (34)$$

Note that $(-k_{14}k_{18}) > 0$. Therefore, the frequency of motion of the fluttering panel is either

$$\bar{\omega}^2 < \min\,(R_1, R_3)$$

or

$$\bar{\omega}^2 > \max\,(R_1, R_3) \qquad (35)$$

It can be concluded that the panel may have two types of deformations. Static deformations given by equation (31) exist if the distribution of temperature is nonuniform. If the temperature is uniformly distributed over the planform of the panel, these deformations vanish within the Galerkin-type analysis. Panel flutter can be superimposed on static deformations at the Mach number given by equation (34). In the numerical example the attention is concentrated on static deflections of the panel at the center; see equations (31)

$$\bar{W} = \sum_n \bar{W}_{1n}^{o} \sin n\pi/2 \qquad (36)$$

which is the largest deflection.

III. Numerical Examples

The cylindrical panel considered in the numerical examples is assumed to be made from boron fiber/Al 7178-T6 matrix composite. The properties of this material at room temperature are E_L = 31 Msi, E_T = 19 Msi, G_{LT} = 6.4 Msi, ν_{LT} = 0.255, α_L = 5.16 μin/in/°F, α_T = 10.1 μin/in/°F.

The calculations were carried out by assumption that T_o = 700°F and the effect of high temperature on mechanical properties is uniform throughout the plate. This assumption imposes limits on the magnitude of a_1a, a_2a, b_1b, b_2b^2 which cannot be too large. Degradation of mechanical properties due to high temperature was calculated based on the data on mechanical properties of boron/aluminum at $T_o = 0$ and $T_o = 700$°F given in reference 11: E_L = 22.3 Msi, E_T = 5.2 Msi, G_{LT} = 1.7 Msi. The Poisson's ratios and the coefficients of thermal extension were assumed to be unaffected by temperature. Circumferential load N_2 was zero in all examples. The panel was formed of 30 layers symmetrically oriented with the lamination scheme 0 ± 45° (two layers adjacent to the middle surface have the lamination angle 0°).

The effect of the Mach number on static deflections of the panel appeared to be negligible. This can be explained by the analysis of the coefficient $\rho_a c^2/E_T$ in k_{14} and k_{18} which has an order of 10^{-6}. Therefore, static deformations are due to aerodynamic heating and only to a negligible degree to aerodynamic pressure. Note that in geometrically nonlinear problems this conclusion may be invalid. In the following examples, the Mach number was always taken as M = 4.

As it can be seen from the solution, temperature change causes transverse deflections only if it is nonuniformly distributed over the planform. In the examples, it was supposed that $a_o = b_o = 1$, $b_1b = b_2b^2 = 0.1$, i.e., temperature was nonuniform in the circumferential direction. The values of a_1a and a_2a^2 were taken equal to either zero or 0.1.

The effect of the panel central angle on static deflections of cylindrical panels is shown in Figs. 2,3. Deflections are always larger in narrower panels; they decrease at larger panel angles (except for the case of very thick panels as illustrated by curve 3 in Fig. 2) and converge to a constant value. This indicates that wide panels behave as closed circular shells of the same geometry. Similar conclusions were obtained by Sobel, Weller, and Agarwal in problems of static buckling of isotropic panels.[12,13] Physically the increase of the deflection in wider panels can be explained by the fact the temperature is "more uniformly" distributed in such panels if $b_1b = b_2b^2$ = const. Apparently, this affects the magnitude of deflections more than the tendency of wider plates to have large deformations due to the smaller effect of the boundary conditions along the straight edges.

The influence of the length-to-radius ratio is illustrated in Figs. 4,5. Deflections of the panels tend to approach zero if their radius increases (small $\bar{a}$). The explanation for this fact is that if the radius increases, the panel approaches a flat plate which has a very small deflection due to nonuniform temperature distribution.

The effect of axial compression is shown in Fig. 6. The deflection curve in all cases considered consists of two branches. At certain values $N_1/N_{cr} < 1$, the deflection approaches infinity, i.e., the panel becomes unstable. The right branch can be reached only if the temperature is applied after the application of compressive load, provided that instability in the transient regime is avoided.

The estimation of the influence of temperature on deflections is shown in Figs. 7,8. The calculations for these figures were carried out by assuming that the mechanical properties of the material remain constant within the range of temperatures considered. The effect of T_o on deflections of relatively thick panels is not very large. However, deflections of thin panels increase at a much higher rate with the increase of temperature (curves 1 in Figs. 7,8).

Finally, the influence of spatial distribution of temperature is shown in Fig. 9. The nonuniform distribution of temperature along the straight edges does not change the character of the deflection versus relative thickness $\bar{h}$ relationship. However, if $b_1b = b_2b^2 = 0$ while $a_1a = a_2a^2 = 0.1$, the magnitude of $\bar{W}$ is of the order of 10^{-3} only (this curve is not shown in Fig. 9). This means

that significant static deflections can exist only if the temperature is nonuniformly distributed along the curved edges.

IV. Conclusions

Deformations of nonuniformly heated composite cylindrical panels in a supersonic gas flow have been considered. It was found that static deflections can be considerable if temperature is nonuniformly distributed over the planform. The effect of aerodynamic pressure on static deformations is negligible compared with the effect of nonuniform aerodynamic heating at high velocities of flight. Significant static deformations can be reached only if temperature is nonuniformly distributed along the curved edges.

As the panel angle is increased, the static deformations approach a constant value which is equal to deformation of a circular cylindrical shell of the same geometry. The deformations are much larger in curved panels than in the shallower panels. There exists, in the presence of the temperature, a critical value of the axial compressive load which is usually much smaller than the classical buckling load calculated in the absence of temperature. The deflection of the panel increases as the temperature is increased. This increase is more pronounced in thinner panels.

References

(1) Ambartsumian, S.A., *General Theory of Anisotropic Shells*, Nauka, Moscow, pp. 430-440, 1974. In Russian.

(2) Librescu, L., *Elastostatics and Kinetics of Anisotropic and Heterogeneous Shell-Type Structures*, Noordhoff, Leyden, The Netherlands, 1975.

(3) Kosichenko, A.A., Pochtman, Yu.M., and Rikards, R.B., "Design of Composite Cylindrical Shells of Minimum Weight in Supersonic Gas Flow," *Soviet Aeronautics*, Vol. 23, 1980, pp. 49-52.

(4) Dixon, S.C., "Experimental Investigation at Mach Number 3.0 of Effects of Thermal Stresses and Buckling on Flutter Characteristics of Flat Single-Bay Panels of Length-Width Ratio 0.96." NASA TN D-1485, 1962.

(5) Novichkov, Yu.N., "Nonstationary Flutter of Cylindrical Panels," *Proceedings of the IV-th All-Union Conference on the Theory of Shells and Plates*, Erevan, 1964. In Russian.

(6) Schaeffer, H.G. and Walter, L.H. Jr., "Flutter of a Flat Panel Subjected to a Nonlinear Temperature Distribution," *AIAA Journal*, Vol. 3, 1965, pp. 1918-1923.

(7) Bolotin, V.V. and Novichkov, Yu.N., "Buckling and Steady Flutter of Heat-Compressed Panels in a Supersonic Flow," NASA TT F-10106, 1966.

(8) Soong, T-C., "Thermoelastic Effect on Delta-Wing Flutter with Arbitrary Stiffness Orientation," *Journal of Aircraft*, Vol. 9, 1972, pp. 835-843.

(9) Bert, C.W. and Reddy, V.S., "Cylindrical Shells of Bimodulus Composite Material," *Journal of the Engineering Mechanics Div., ASCE*, Vol. 108, 1982, pp. 675-688.

(10) Almroth, B.O., "Influence of Edge Conditions on the Stability of Axially-Compressed Cylindrical Shells," *AIAA Journal*, Vol. 4, 1966, pp. 134-140.

(11) *Advanced Composite Design Guide*, Vol. IV, 3rd ed., Structures Division, Air Force Flight Dynamics Laboratory, Wright-Patterson AFB, Ohio, 1973.

(12) Sobel, L.H., Weller, T., and Agarwal, B.L., "Buckling of Cylindrical Panels under Axial Compression," *Computers and Structures*, Vol. 6, 1976, pp. 29-35.

(13) Weller, T., "Combined Effects of In-Plane Boundary Conditions and Stiffening on Buckling of Eccentrically Stringer-Stiffened Cylindrical Panels," *Computers and Structures*, Vol. 14, 1981, pp. 427-442.

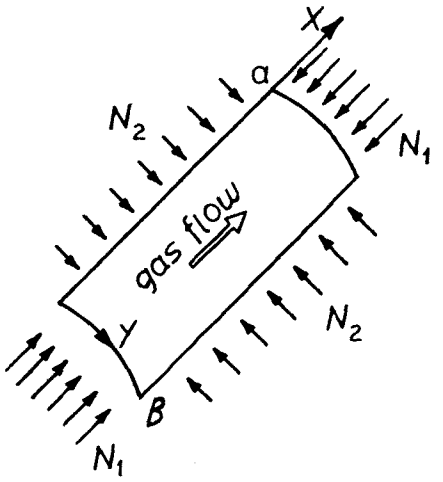

Figure 1. Cylindrical Panel in a Gas Flow

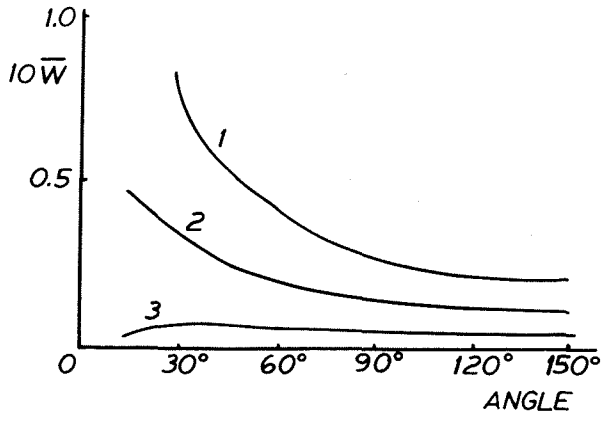

Figure 2. Effect of Panel Included Angle on Static Deflection ($\bar{a} = 0.5$; $a_1 a = a_2 a^2 = 1$; $N_1 = 0$). Curves 1, 2, and 3 correspond to dimensionless thicknesses $\bar{h}$ of 0.01, 0.02, and 0.05, respectively

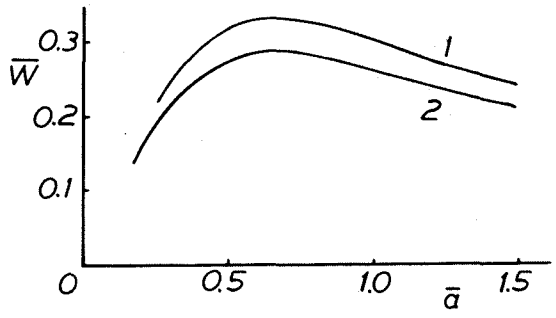

Figure 4. Effect of Length-to-Radius Ratio on Static Deflection ($\bar{h} = 0.01$; $\lambda = 2$; $N_1 = 0$). Curves 1 and 2 correspond to values of $a_1 a = a_2 a^2$ of 0 and 0.1, respectively

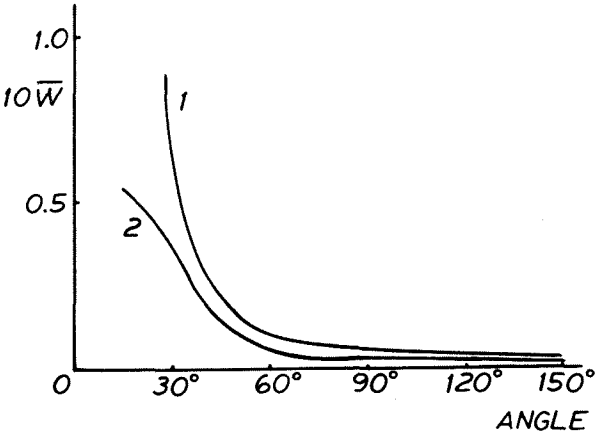

Figure 3. Effect of Panel Included Angle on Static Deflection ($\bar{a} = 0.5$; $a_1 a = a_2 a^2 = 0$; $N_1 = 0$). Curves 1 and 2 correspond to dimensionless thicknesses $\bar{h}$ of 0.01 and 0.02, respectively

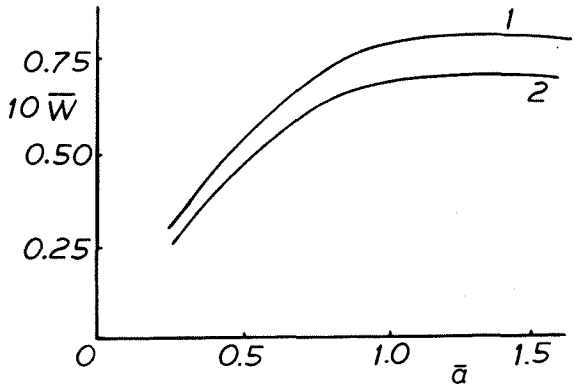

Figure 5. Effect of Length-to-Radius Ratio on Static Deflection ($\bar{h} = 0.02$; $\lambda = 2$; $N_1 = 0$). Curves 1 and 2 correspond to values of $a_1 a = a_2 a^2$ of 0 and 0.1, respectively

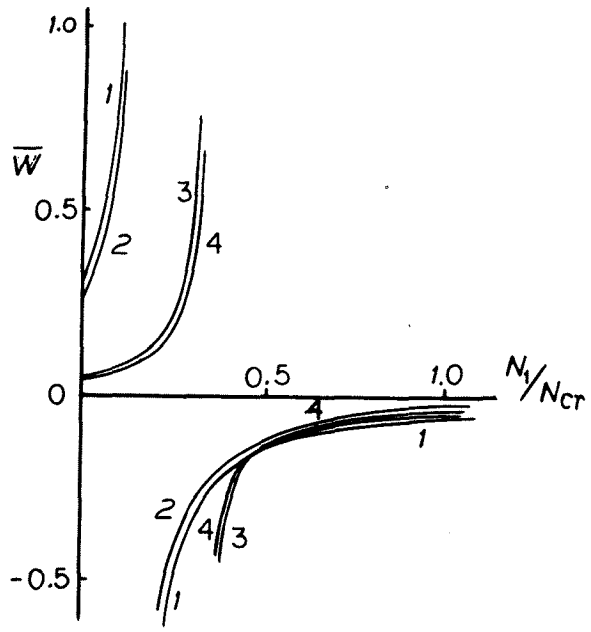

Figure 6. Effect of Dimensionless Axial Compression on Static Deflection ($\lambda = 2$). Curves 1 and 2 correspond to $a_1 a = a_2 a^2$ values of 0 and 0.1, with $\bar{h} = 0.01$ for both; curves 3 and 4 correspond to $a_1 a = a_2 a^2$ values of 0 and 0.1, with $\bar{h} = 0.02$ for both

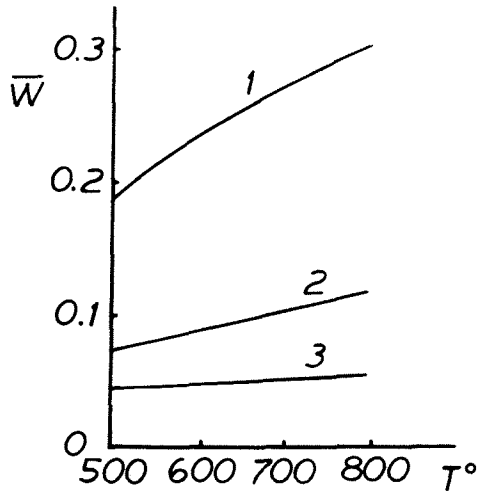

Figure 8. Effect of Temperature on Static Deflection ($\bar{a} = 0.05$; $\lambda = 2$; $a_1 a = a_2 a^2 = 0.1$; $N_1 = 0$). Curves 1, 2, and 3 correspond to dimensionless thicknesses of 0.010, 0.015, and 0.020, respectively

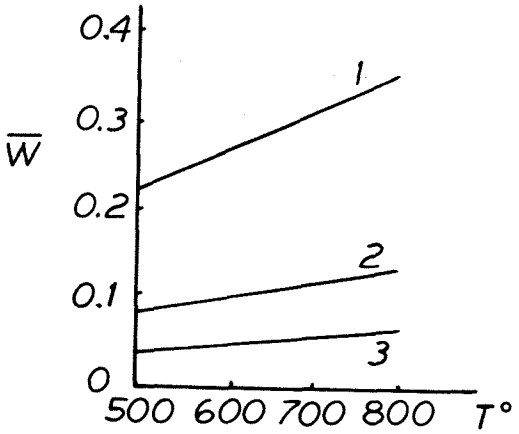

Figure 7. Effect of Temperature on Static Deflection ($\bar{a} = 0.5$; $\lambda = 2$; $a_1 a = a_2 a^2 = 0$; $N_1 = 0$). Curves 1, 2, and 3 correspond to dimensionless thicknesses of 0.010, 0.015, and 0.020, respectively

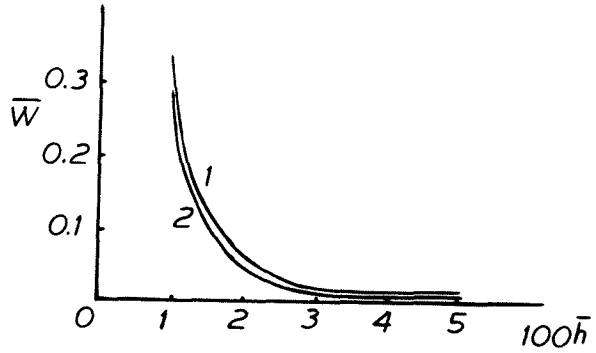

Figure 9. Effect of Spatial Distribution of Temperature on Static Deflection ($\bar{a} = 0.5$; $\lambda = 2$; $N_1 = 0$). Curves 1 and 2 correspond to values of $a_1 a = a_2 a^2$ of 0 and 0.1, respectively